Research Article | Vol. 25, No. 2 | 23 Jan 2017 | OPTICS EXPRESS 1040

Optics EXPRESS

Strong hybridization of edge and bulk states in dimerized PT-symmetric coupled waveguide chain

Bei Wu,[1] Jiamin Wang,[1] Meng Xiao,[2] Jing Xu,[1,3] and Yuntian Chen[1,3,*]

[1]*School of Optical and Electronic Information, Huazhong University of Science and Technology, Wuhan, China*
[2]*Department of Physics, The Hong Kong University of Science and Technology, Hong Kong, China*
[3]*Wuhan National Laboratory of Optoelectronics, Huazhong University of Science and Technology, Wuhan, China*
[*]*yuntian@hust.edu.cn*

Abstract: We study mode coupling of an edge state with bulk states in a coupled waveguide chain in the presence of gain and losses. In a low non-Hermiticity regime, it is found that the edge state associated with the interface between two topologically different waveguide chains is well isolated from the bulk states, sharing the exact same features as the well-known Su-Schrieffer-Heeger Model. As the non-Hermiticity increases, the two bands of the overall waveguide chain merge together, which leads to the overlap in the band diagram between the edge state and states of lower bands. We find that before the PT-symmetry breaking, the edge state is strongly coupled to bulk states of lower bands, evident by the anti-crossing feature in the band diagram. The strong mode hybridization is verified by a non-Hermitian coupled mode theory developed from reaction conservation, and is further examined using phenomenological models. We envisage that the strong coupling between the edge state and the bulk state may be useful in expanding our understanding in topological photonics in non-Hermitian condition, as well as in applications such as mode conversion between edge and bulk states.

OCIS codes: (230.7370) Waveguides; (080.1238) Array waveguide devices; (350.1370) Berry's phase.

References and links

1. C. L. Kane and E. J. Mele, "Z_2 topological order and the quantum spin Hall effect," Phys. Rev. Lett. **95**(14), 205414 (2005).
2. M. Z. Hasan and C. L. Kane, "Colloquium: topological insulators," Rev. Mod. Phys. **82**(4), 3045–3067 (2010).
3. X. L. Qi and S. C. Zhang, "Topological insulators and superconductors," Rev. Mod. Phys **83**(4), 175–179 (2011).
4. S. Q. Shen, "Topological insulators: Dirac equation in condensed matters," Springer Series in Solid-State Sciences **174** (2012).
5. S. Ryu and Y. Hatsugai, "Topological origin of zero-energy edge states in particle-hole symmetric systems," Phys. Rev. Lett. **89**(7), 077002 (2002).
6. R. Mong and V. Shivamoggi, "Edge states and the bulk-boundary correspondence in Dirac Hamiltonians," Phys. Rev. B **83**, 125109 (2011).
7. M. Xiao, Z. Q. Zhang, and C. T. Chan, "Surface impedance and bulk band geometric phases in one-dimensional systems," Phys. Rev. X **4**, 021017 (2014).
8. C. W. Ling, M. Xiao, C. T. Chan, S. F. Yu, and K. H. Fung, "Topological edge plasmon modes between diatomic chains of plasmonic nanoparticles," Opt. Express **23**, 2021–2031 (2015).
9. X. Q. Huang, M. Xiao, Z. Q. Zhang, and C. T. Chan, "Sufficient condition for the existence of interface states in some two-dimensional photonic crystals," Phys. Rev. B **90**(7), 075423 (2014).
10. W. P. Su, J. R. Schrieffer, and A. J. Heeger, "Solitons in polyacetylene," Phys. Rev. Lett. **42**(25), 1698–1701 (1979).
11. W. P. Su, J. R. Schrieffer, and A. J. Heeger, "Soliton excitations in polyacetylene," Phys. Rev. B **22**(4), 2099–2111 (1980).
12. D. J. Thouless, M. Kohmoto, M. P. Nightingale, and M. Den Nijs, "Quantized Hall conductance in a two-Dimensional periodic potential," Phys. Rev. Lett. **49**(6), 405 (1982).
13. Y. Ando, "Topological insulator materials," J. Phys. Soc. Jpn. **82**(10), 102001 (2013).
14. S. Ho, F. Lin, and X. Wen, "Majorana zero-modes and topological phases of multi-flavored Jackiw-Rebbi model," J. High Energy Phys. 07412 (2012).

#279718 http://dx.doi.org/10.1364/OE.25.001040
Journal © 2017 Received 31 Oct 2016; revised 16 Dec 2016; accepted 20 Dec 2016; published 12 Jan 2017

Optics EXPRESS

15. D. G. Angelakis, P. Das, and C. Noh, "Probing the topological properties of the Jackiw-Rebbi model with light," Sci. Rep. **4**, 6110 (2014).
16. A. B. Khanikaev, S. H. Mousavi, W. K. Tse, M. Kargarian, A. H. Macdonald, and G. Shvets, "Photonic topological insulators," Nat. Mater. **12**(3), 233–239 (2012).
17. W. J. Chen, "Experimental realization of photonic topological insulator in a uniaxial metacrystal waveguide" Nat. Commun. **5**, 6782:1–7 (2014).
18. Y. Hatsugai, "Chern number and edge states in the integer quantum Hall effect," Phys. Rev. Lett. **71**(22), 3697–3700 (1993).
19. P. Delplace, D. Ullmo, and G. Montambaux, "Zak phase and the existence of edge states in graphene," Phys. Rev. B **84**, 195452 (2011).
20. D. Guzman-Silva, C. Mejia-Cortes, M. A. Bandres, M. c. Rechtsman, S. Weimann, S. Nolte, M. Segev, A. Szameit, and R. A. Vicencio, "Experimental observation of bulk and edge transport in photonic Lieb lattices," New J. Phys. **16**(6), 063061 (2014).
21. X. F. Zhu, Y. G. Peng, X. Y. Yu, H. Jia, M. Bao, Y. X. Shen, and D. G. Zhao, "Topologically protected acoustic helical edge states and interface states in strongly coupled metamaterial ring lattices," arXiv:1508.06243 (2015).
22. R. Fleury, A. B. Khanikaev, and A. Al, "Floquet topological insulators for sound," Nat. Commun. **7**, 11744 (2016).
23. C. He, X. Ni, H. Ge, X. C. Sun, Y. B. Chen, M. H. Lu, X. P. Liu and Y. F. Chen, "Acoustic topological insulator and robust one-way sound transport," Nat. Phys. (2015).
24. P. Wang, L. Lu, and K. Bertoldi, "Topological phononic crystals with one-way elastic edge waves," Phys. Rev. Lett. **115**, 104302 (2015).
25. Z. Wang, Y. Chong, J. Joannopoulos, and M. Soljai, "Reflection-free one-way edge modes in a gyromagnetic photonic crystal," Phys. Rev. Lett. **100**(1), 145–150 (2008).
26. K. X. Liu, L. F. Shen, and S. He, "One-way edge mode in a gyromagnetic photonic crystal slab," Opt. Lett. **37**(19), 4110-4112 (2012).
27. H. Zhao, S. Longhi, and L. Feng, "Robust light state by quantum phase transition in non-Hermitian optical materials," Sci. Rep. **5**, 17022 (2015).
28. S. Maizard, C. Poli, and H. Schomerus, "Topological protected defect states in open photonic systems with non-Hermitian charge-conjugation and parity-time symmetry," Phys. Rev. Lett. **115**, 200402 (2015).
29. T. E. Lee, "Anomalous edge state in a non-Hermitian lattice," Phys. Rev. Lett. **116**, 133903 (2016).
30. J. Xu and Y. Chen, "General coupled mode theory in non-Hermitian waveguides," Opt. Express **23**(17), 22619–22627 (2015).
31. COMSOL MULTIPHYSICS 5.2 (2015). COMSOL Multiphysics: a finite element analysis, solver and simulation software for various physics and engineering application, especially coupled phenomena, or multiphysics. URL http://www.comsol.com/.
32. Z. Z. Liu, Q. Zhang, X. L. Liu, Y. Yao, and J. J. Xiao, "Absence of exceptional points in square waveguide arrays with apparently balanced gain and loss," Sci. Rep. **6**, 22711 (2016).

1. Introduction

Edge states emerge at the interfaces formed by two topologically distinct bulk materials [1–4]. And the number of the edge states is determined by the topological invariant for each individual band associated with different bulk materials. The link between the number of the edge states and the topological properties of the bulk materials, i.e., topological invariant, is coined as bulk-edge correspondence, which is discovered in mathematics and found further applications in quantum field theory, condense matter physics, as well as optics [5–9]. Thank to such theorem, a number of models and interesting phenomena, such as the Su-Schrieffer-Heeger (SSH) model for polyacetylene [10,11] , quantum Hall effect (TKNN invariant) [12,13], Jackiw-Rebbi model [14,15], topological insulator [16,17] and many others, can be explained in a unified but concise manner.

The connection between the existence of the edge states and bulk properties has been investigated extensively in electronics, acoustics, and optics [18–23]. Very much attention is drawn to designing particular structures that fulfill certain requirements, to favor or forbid the existence of edge states. Ideally, those edge states are 'isolated' such that they don't interact with bulk states, as well as other edge states with different propagation direction (time reversal partner) or different polarization, which eventually leads to many interesting features, such as one-way transportation, back-scattering immunity, or optical diode [22–26]. All the aforementioned features about the edge states apply for the Hermitian bulk system without any imperfections.

Practically, one edge state may be possibly coupled to bulk modes or the edge state on the

Optics EXPRESS

opposite edge. Indeed, a 'magnetic' scatter can give rise to scattering of the spin edge state in topological insulator, making it couple to the oppositely propagating state. In non-Hermitian settings, it is found that much more is involved. As an example, the system with parity-time (P-T) symmetry is one of typical types of non-Hermitian systems. In optics, PT-symmetric system needs the refractive index with the space distribution $n(x) = n^*(-x)$ (* respects complex conjugation). In such system, the eigenvalue spectrum is still real with smaller non-Hermiticity, while with large enough non-Hermiticity, the real spectrum bifurcates into complex plane. In recent years, there are several papers about PT-symmetric systems with edge states and their properties. Zhao and co-authors found that robust light states exist due to the PT-symmetric transition in non-Hermitian optical materials [27]. Malzard and co-authors found that topologically protected edge states exist in non-Hermitian system, while disappear in the corresponding Hermitian limit [28]. Interestingly, Tony Lee pointed out that in one-dimensional non-Hermitian lattice system, the topological invariant becomes fractional, which may lead to further modification of bulk edge correspondence in general non-Hermitian settings [29].

In this paper, we show that at low non-Hermitian regime, the edge states of a dimerized waveguide chain exist regardless of whether the overall structure respect PT-symmetry globally or not. We further show that the edge and bulk states can be strongly coupled, yielding anti-crossing feature as the non-Hermiticity increases. The mode hybridization between the edge and bulk states is due to the presence of non-Hermiticity, leading the merging of lower and upper bands, that inevitably gives rise to the overlapping of the edge state and bulk band states in the band diagram. Due to the presence of the strong coupling between the bulk states and edge states, those states may be adiabatically converted into each other in a judiciously designed PT-symmetric waveguide chain. Our results are further verified by a non-Hermitian coupled mode theory developed before [30].

The paper is organized as follows. In Section 2, we analyze the properties bulk states in dimerized PT-symmetric waveguide chains. In section 3, we study the edge state in waveguide chain with and without global PT-symmetry. It is found that the edge state exists in lower non-Hermiticity regime, and interacts strongly with the bulk states in high non-Hermiticity regime. In section 4, we study the strong modal hybridization between the edge state and the bulk states using a non-Hermitian coupled equation, as well as using phenomenological model. Lastly, Section 5 concludes the paper.

2. Bulk properties of the dimerized PT-symmetric waveguide chains

We examine the properties of the bulk states of dimerized PT-symmetric waveguide chains, in analogy to the SSH model, as shown in Fig. 1. In contrast to the SSH model, we replace the carbon atoms with single-mode waveguides. The width and height of the single-mode waveguide are given by $w = 0.3\lambda_0$ and $h = 0.1\lambda_0$, λ_0 being vacuum wavelength, from which one obtain the effective refractive index of the single-mode waveguide $n^0_{eff} = 1.51$. To form a dimerized waveguide lattice, each unit cell consists of two identical single-mode waveguides, where d is the distance between the two waveguides, and D is the lattice constant. Depending on $d > D/2$ or $d < D/2$, The interaction of waveguides inside each unit cell can be taken as long bond or short bond in analogy to the SSH model. We study two different coupled waveguide lattices in Fig. 1, denoted by waveguide lattice A and B respectively. The waveguide lattice A and B share all the same geometrical parameters, except that the periodicity D differs. Specifically, the periodicity D of lattice A equals to $1.2\lambda_0$, while the periodicity D of lattice B equals to $1.3\lambda_0$. In both A and B structures, $d = 0.8\lambda_0$. The relative permittivities of two waveguides are given by $\epsilon_r = \epsilon_r^0 \pm i\Delta\epsilon$ to respect PT symmetry, indicated by red (gain) and blue (loss) rectangles shown in the insert of Figs. 1(b) and 1(e). The band structures as well as the modes of periodic waveguide chains are calculated using a commercial software package, COMSOL MULTIPHYSICS 5.2 [31].

Optics EXPRESS

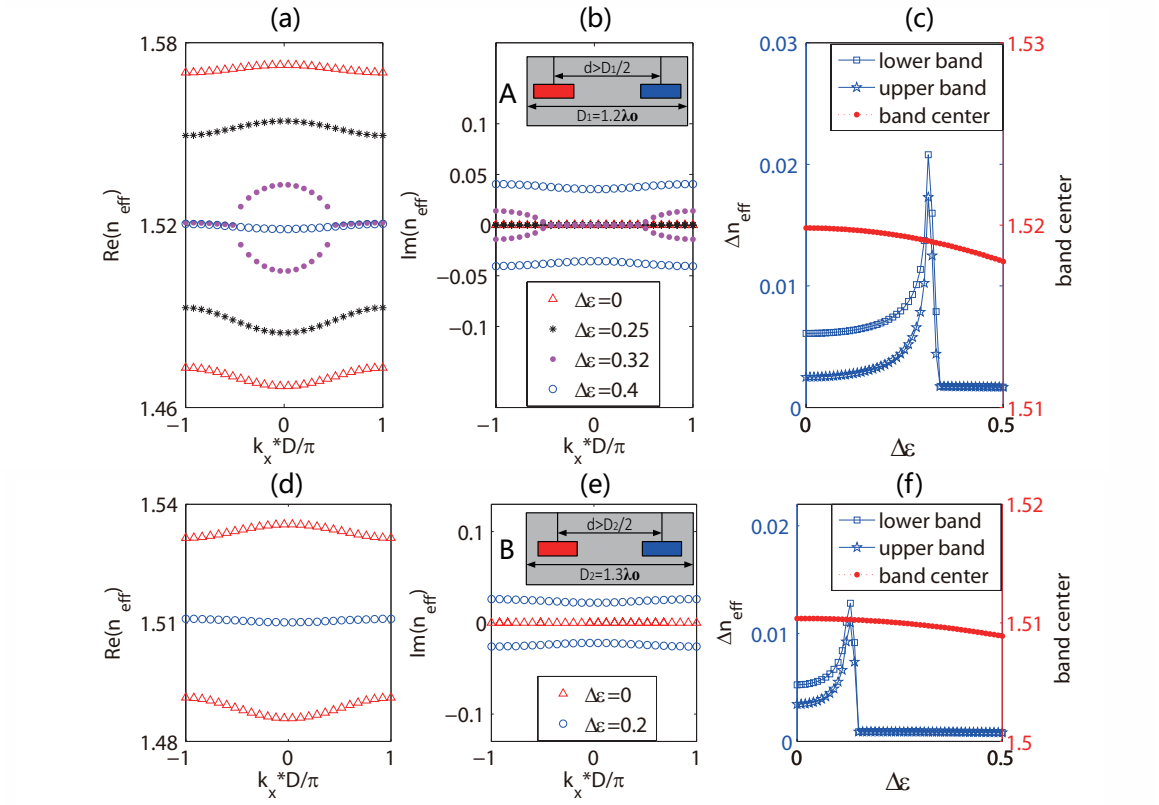

Fig. 1. Bulk properties of the dimerized PT-symmetric waveguide lattices A and B. Each unit cell contains two identical single-mode waveguides with width and height denoted by w and h. The working wavelength is λ_0, and the relative permittivity of single-mode waveguide core is $\epsilon_r^0 = 10$, embedded in air cladding. (a)–(b)/(d)–(e) show the real part and imaginary part of eigenvalues of band structure with four values of $\Delta\epsilon$ for waveguide lattice A/B. (c)/(f) shows the width of the projected band Δn_{eff} and the band-center as function of non-Hermiticity $\Delta\epsilon$.

In Figs. 1(a)–1(c), the band structures of waveguide lattice A, i.e., the effective refractive index (denoted as n_{eff} onward for short) of these dimerized waveguide chains are calculated for four different $\Delta\epsilon$ ($\Delta\epsilon = 0, 0.25, 0.32, 0.4$), from which we will discuss the properties of bulk state involution as non-Hermiticity increases. Firstly, at $\Delta\epsilon = 0$, the waveguide lattice is Hermitian and has real eigenvalues, i.e., $Im(n_{eff}) = 0$, evident by red triangles shown in Figs. 1(a) and 1(b). In this phase, the topological properties of the wave function associated with the lower and upper bands of the coupled waveguide lattice share the exact same feature as the SSH model. From full-wave simulation, one find the Zak phases of the lower and upper bands are 0 for short bond structure, while Zak phases are π for long bond structure, indicating the existence of distinct topological phases between two cases, i.e., the structure parameter $d < D/2$ and $d > D/2$. Secondly, at $\Delta\epsilon = 0.25$, the eigenvalues of the waveguide lattice, i.e., n_{eff}, remains real, thus one can expect that it shares similar topological features as $\Delta\epsilon = 0$. As the non-Hermiticity increases up to $\Delta\epsilon = 0.32$, one can find that the lower band and upper bands merge together at larger Bloch k-vector. Meanwhile, the imaginary part of n_{eff} splits. This is exactly the same as the PT-symmetry breaking phenomenon, with the parameter space being the Bloch k-vector, rather than being $\Delta\epsilon$ which directly quantifies the non-Hermiticity. Lastly, it

Optics EXPRESS

is found that at $\Delta\epsilon = 0.4$, the real parts of n_{eff} of the lower and upper bands overlap completely, while imaginary parts of n_{eff} are split throughout the Brillouin zone. From the viewpoint of the PT symmetry, We note that the aforementioned bulk state properties with different $\Delta\epsilon$ can be classified as unbroken phase, half-broken phase, and completely broken phase as discussed in [27].

In Figs. 1(d)–1(f), the band structure of the waveguide lattice B is studied. The red triangles (blue circles) in Figs. 1(d) and 1(e) shows the two bands for $\Delta\epsilon = 0$ ($\Delta\epsilon = 0.2$), which corresponds to the unbroken phase (completely broken phase). Together with other values $\Delta\epsilon$ (not shown here), we find that the band properties of the waveguide lattice share the similar features as that of Figs. 1(a) and 1(b), which depends on $\Delta\epsilon$ and can be classified into three phases. However, there is few subtle differences in the band center and the width of the projected upper and lower bands of the two waveguide lattices, shown in Figs. 1(c) and 1(f). The left y-axis in panel (c)/(f) shows the band-width of the projected upper and lower bands in waveguide lattice A/B, while the right y-axis shows the band-center between upper and lower bands at $k_x = 0$ in waveguide lattice A/B. In Figs. 1(c) and 1(f), one find that the changing of the band width of two bands have the same tendency. The two band width increase at first, and then suddenly reduce to a certain value with large enough $\Delta\epsilon$, and finally remain unchanged. As regards to the band center, one can realize that band-center denoted by n^c_{eff} in waveguide lattice A, i.e., $n^c_{eff,A} = 1.52$, is larger than that of waveguide lattice B, which approximately equals to the modal index of single waveguide($n^c_{eff,B} = n^0_{eff}$). The rationale behind the subtle difference between $n^c_{eff,A}$ and $n^c_{eff,B}$, with respect to n^0_{eff}, is the following: (1) the field distribution of upper band in waveguide lattice A is largely concentrated in a tiny gap with width of $0.1\lambda_0$, which gives rise to a larger effective modal index of the upper band. Meanwhile, the field distribution of the lower band is largely concentrated in the waveguide core medium. Thus, the overall effect of the field re-distribution gives rise to a up-ward shift of the band-center, as shown in Fig. 1(c); (2) as for waveguide lattice B, the fields of the lower and upper bands mostly remain inside the waveguide core, therefore the band-center coincides with n^0_{eff}. The relatively large difference between $n^c_{eff,A}$ and n^0_{eff}, which turns out to be necessary to obtain the strong coupling between the edge state and the bulk states, will be discussed in the following section.

3. Edge state in a non-Hermitian waveguide chain

In Hermitian waveguide lattice structure with infinite periods, i.e., $\Delta\epsilon = 0$, there is a topological transition of the wavefunction for each band as the distance of the two waveguides d crosses $D/2$, which separates two distinct topological phases denoted by difference Zak phases, one is π and the other is 0. Interestingly, the mode properties of waveguide lattice structure with finite length, which will be referred as waveguide chains onward, crucially depends on bulk state properties of waveguide lattice. For a one-dimensional (1D) waveguide chain containing even number, i.e., 2N, single-mode waveguides, there are basically two options to group the single-mode waveguides into N unit cells, which can be either N short-bond unit cells or N long-bond unit cells. Due to topological reasons, there is no edge states associated with the waveguide chain that only contains short-bond unit cells. However, for a waveguide chain that only contains long-bond unit cells, there are two edge states localized at the two ends of the waveguide chain, due to the difference of the topological phases at the interface between the waveguide chain and air. When the chain is of finite length, two edge states interact with each other and split into an even mode and an odd mode. The splitting is quite small as both modes locate inside the bulk band gap region. As the length of waveguide chain becomes infinite, the splitting will go to zero. For a non-Hermitian long-bond waveguide chain, one can immediately realize that the two edges become PT-symmetric broken even though the perturbation of the non-Hermiticity $\Delta\epsilon$ is very small, due to the very small difference of n_{eff} between the two edge

Optics EXPRESS

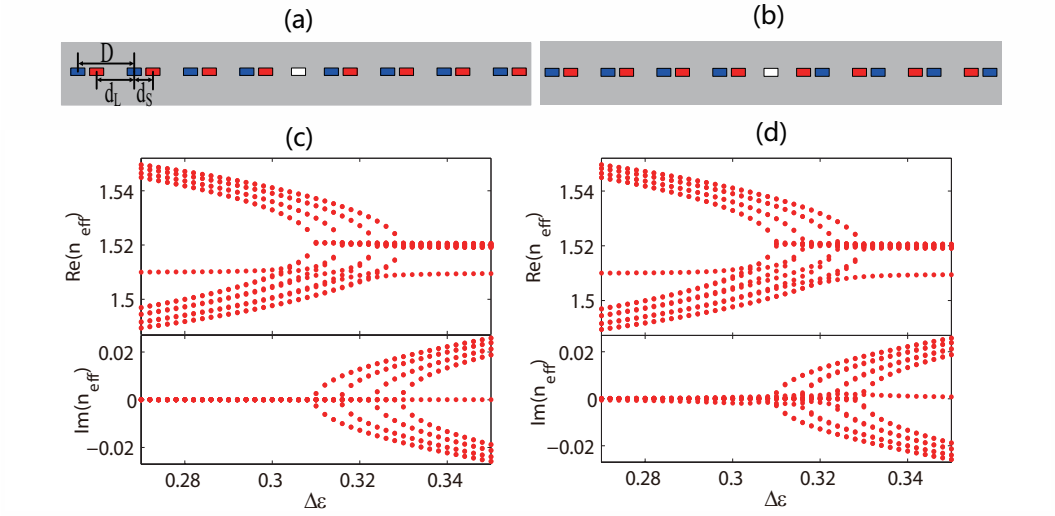

Fig. 2. Edge state in coupled waveguide chains with global PT symmetry and local PT symmetry which consist of seventeen waveguides. (a) is the structure of PT symmetric waveguide chain with the condition $n(x) = n^*(-x)$, and $x = 0$ is the center of the structure. The larger space between two waveguides $d_L = 0.8\lambda_0$, the smaller one $d_S = 0.4\lambda_0$ and the periodicity $D = 1.2\lambda_0$. (b) is the structure of waveguide chain with local PT symmetry and mirror symmetry. Local PT symmetry is in the unit cell with two waveguides and mirror symmetry means $n(x) = n^*(-x)$ with the center of the structure. (c) and (d) show the band dispersion of the structure in (a) and (b), respectively.

states.

In this paper, we intend to explore how the non-Hermiticity impacts the edge state, thus we study the waveguide chain that contains odd number ($4N + 1$ and N is an integer) single mode waveguides in total to avoid the complication of the mode coupling between edge states. The 1D waveguide chains sketched in Figs. 2(a) and 2(b) can be considered as one waveguide chain with N short-bond unit cells, in combination with another waveguide chain that contains $N + 1/2$ unit cells, and $N = 4$ as an example. In Figs. 2(a) and 2(b), the coupled waveguide chain only supports one edge state, and preserves the local PT-symmetry at the meantime. The local PT-symmetry here refers to the fact that refractive indices $n(x)$ in the unit cell obey the PT symmetric conditions, i.e., $\mathtt{Re}(n(x)) = \mathtt{Re}(n(-x))$ and $\mathtt{Im}(n(x)) = -\mathtt{Im}(n(-x))$, with respect to the mirror plane in the center of the unit cell. Specifically, the chains in Fig. 2 comprise two parts with seventeen waveguides. The left part ends with long bond composed of nine waveguides, and the right part starts with short bond composed of eight waveguides, thus the edge state appears in the ninth waveguides which can been seen as an interface. Globally, the coupled waveguide chains can be either PT symmetric or PT-symmetry broken, which are corresponding to the structures in Figs. 2(a) and 2(b), respectively. The structure on the left is PT symmetric which called GPT for short, and the other one on the right is local PT symmetric called LPT. Red (blue) rectangles stand for waveguides with gain (losses). The white one is the waveguide without gain and losses. In Fig. 2, the periodicity D of one unit cell is $1.2\lambda_0$, and the smaller space and larger space between two waveguides in one unit cell are $d_S = 0.4\lambda_0$ and $d_L = 0.8\lambda_0$, as same as the parameters of the unit cell in the inset of Fig. 1(b).

From topological argument, one can expect that an edge state exists between the waveguide chains with different Zak phases. As shown in Figs. 2(c) and 2(d), it can be found that there are several similarities between the GPT and LPT structures. In low non-Hermiticity regime,

Optics EXPRESS

i.e., $\Delta\epsilon < 0.3$, the edge state exists in GPT structure as well as in LPT structure. The existence of edge state at lower Hermiticity is ensured by sub-lattice symmetry in the waveguide chain, regardless of the global PT-symmetric property of the overall structure. Apparently, the edge state is robust in the presence of lower non-Hermiticity, i.e., $\Delta\epsilon < 0.3$, evident by the relatively large bandgap between the edge state and bulk states, as shown in Figs. 2(c) and 2(d). Apart from those similarities, there are still few distinctions in the band-diagram between GPT structure and LPT structure. Firstly, there is a clear transition point, namely, the exceptional point, where the PT-symmetric breaking occurs in GPT structure. In contrast, there is no such sharp transition point in LPT structure. The absence of exceptional points is due to the lack of the exact global PT-symmetry, which is different from the scenarios where the asymmetric coupling plays a role [32]. Secondly, the imaginary parts of n_{eff} of the edge state in GPT structure is exactly 0, the imaginary parts of n_{eff} of the LPT waveguide chain fluctuate around zero. Those distinctions indicate that the edge state of the GPT system is more robust than that of the LPT system, although the edge state can emerge in both structures.

We also note the fact that the edge state inevitably intersects with the bulk states from the lower bands for a number of times in Figs. 2(c) and 2(d). The rationale behind such an inevitable intersection is the following: Firstly, the edge state is located in the band gap and is rather isolated from the bulk states, with the effective modal index given by n^0_{eff}. We also note that the effective modal index of the edge state is flat as non-Hermiticity increases; Secondly, as discussed in the previous section, the band-center of the waveguide lattice ($D = 1.2\lambda_0$) is shifted upward ($n^c_{eff,A} > n^0_{eff}$), which is actually the location where the upper and lower bands merger together after the exceptional point; Lastly, one can immediately conclude that the edge state has to intersect with the lower bands, as non-Hermiticity increases. In Fig. 2(c), the edge state anti-crosses the lower band four times, which is equal to half of the number of pairs of waveguide chain, as well as half of the number of the modes in the lower band of the overall structure. In order to have a close look at the mode hybridization, i.e., the anti-crossing between the edge state and bulk states, we proceed to discuss a waveguide chain containing 5 guides in total using phenomenological model and non-Hermitian coupled mode formalism in the next section.

4. Anti-crossing of the edge state with bulk states

4.1. General coupled mode theory in waveguide chain

In this section, we study mode coupling between edge state and bulk states in a simplified structure that consists of five single-mode waveguides. The results in Figs.3(a) and 3(b) are obtained from two independent approaches, blue circles obtained with COMSOL simulation, red stars obtained from non-Hermitian coupled mode equation denoted by GCMT [30]. Figure 3(a)(Figure 3(b)) show real (imaginary) part of effective modal index n_{neff} as a function of non-Hermiticity. In such a simple structure, we can see clearly that there is a strong mode hybridization between the edge state and the bulk states from the lower bands, which is similar to Fig. 2(a) and will be re-examined using GCMT. Figure 3(c) sketches two options of the edge state intersecting with the bulk states: either crossing or anti-crossing as non-Hermiticity increases. From the full-wave simulation indicated by the black box in Fig. 3(a), one can see that the edge state couples to the bulk modes in non-trivial way, featuring as anti-crossing shown in Fig. 3(c2).

We proceed to discuss the non-trivial mode coupling between the edge state and bulk states using non-Hermitian coupled mode formalism. Based on GCMT in [30], we can get the coupling equation as follows,

$$\sum\nolimits_j a_j(\beta - \beta_{0,j})p_{ij} = \sum\nolimits_j a_j k_{ij}, \tag{1}$$

Optics EXPRESS

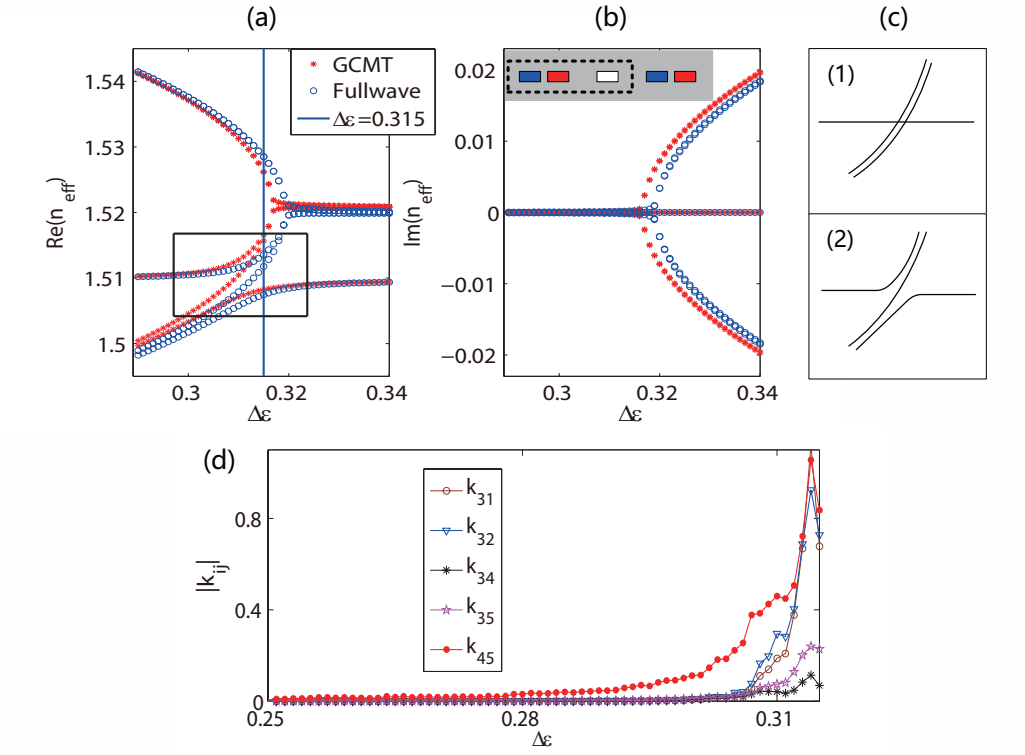

Fig. 3. Band structure and mode evolution sketch of waveguide chain with five waveguides. (a) and (b) show the real and imaginary part of band dispersion in coupled waveguide chains with global PT symmetry which consist of five waveguides, respectively. Blue circles represent the eigenvalues from COMSOL, and red stars represent the eigenvalues from GCMT. (c) The mode evolution in the mode crossing regime, i.e., the black rectangle in (a). (d) The values of k_{31}, k_{32}, k_{34}, k_{35} and k_{45} with varying $\Delta\epsilon$.

where $p_{ij} = \int\int \boldsymbol{z}\cdot(\boldsymbol{e}^{-}_{0,j}\times\boldsymbol{h}^{+}_{0,i}) - \boldsymbol{z}\cdot(\boldsymbol{e}^{+}_{0,i}\times\boldsymbol{h}^{-}_{0,j})dxdy$, $k_{ij} = -k_0\int\int\Delta\epsilon(x,y)\boldsymbol{e}^{-}_{0,j}\cdot e^{+}_{0,i}dxdy$, $\boldsymbol{e}^{\pm}_{0,i}$ ($\boldsymbol{h}^{\pm}_{0,i}$) correspond to the electric (magnetic) field of the ith mode without perturbation in the transverse cross section for forward (+) and backward (−) propagation, and more details refer to [30]. 0 and $i(j)$ represent no perturbation case and mode labels, respectively. a_j is the coupled amplitude with the unperturbed field of the adjoint system. $\beta_{0,j}$ and β are eigenvalues of no perturbation case and perturbation case, respectively. It also can be rewritten in the form of eigenvalue problem. Based on Eq. (1), the coupled mode equation of five single-mode waveguides chain in our study can be explicitly written out as follows,

$$\begin{bmatrix} h_{11} & h_{12} & h_{13} & h_{14} & h_{15} \\ h_{21} & h_{22} & h_{23} & h_{24} & h_{25} \\ h_{31} & h_{32} & h_{33} & h_{34} & h_{35} \\ h_{41} & h_{42} & h_{43} & h_{44} & h_{45} \\ h_{51} & h_{52} & h_{53} & h_{54} & h_{55} \end{bmatrix} \begin{bmatrix} a_1 \\ a_2 \\ a_3 \\ a_4 \\ a_5 \end{bmatrix} = n_{eff}k_0 \begin{bmatrix} p_{11} & p_{12} & p_{13} & p_{14} & p_{15} \\ p_{21} & p_{22} & p_{23} & p_{24} & p_{25} \\ p_{31} & p_{32} & p_{33} & p_{34} & p_{35} \\ p_{41} & p_{42} & p_{43} & p_{44} & p_{45} \\ p_{51} & p_{52} & p_{53} & p_{54} & p_{55} \end{bmatrix} \begin{bmatrix} a_1 \\ a_2 \\ a_3 \\ a_4 \\ a_5 \end{bmatrix}, \quad (2)$$

where $h_{ij} = \beta_j p_{ij} - ik_{ij}$, i/j labels the five waveguide modes under study, and a_j (β_j) refers to the mode amplitude (propagation constant) of j mode for the perturbed system, n_{eff} is modal index of perturbation system. Specifically, i and j label the 5 modes, n_{eff} of which increases as i/j increases, as shown in Fig. 3(a). For instance, mode label $i = 3$ refers to the edge state.

Optics EXPRESS

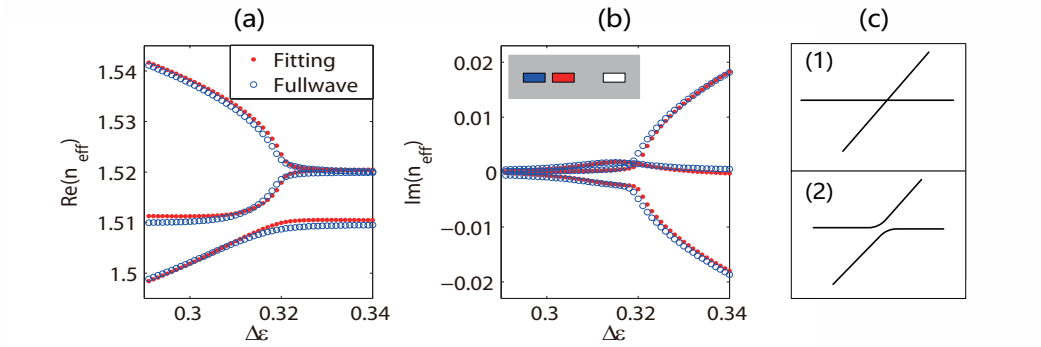

Fig. 4. Band structure and the sketch of mode evolution of waveguide chain with three waveguides. (a/b) shows the real (imaginary) part of band dispersion in coupled waveguide chains. Blue circles represent the eigenvalues from full-wave simulation, and Red dots represent results from phenomenological models. (c) The mode evolution of two mode intersection.

Essentially, Eq. (2) gives the mode hybridization in the full system under a small perturbation from $\Delta\epsilon$, marked as red stars in Figs. 3(a) and 3(b). As can be seen, the n_{eff} obtained from GCMT agrees well with those from the full-wave simulation. There also exists an edge state in band dispersion, which anti-crosses with bulk states. Evident in Eq. (2), it is the term k_{ij} that reflects the interaction among the relevant states. In Fig. 3(a), one can see that the edge state couples strongly with the two states from the lower bands at $\Delta\epsilon \geq 0.3$, where the coupling coefficients k_{31} and k_{32} become significant. Indeed, Fig. 3(d) shows the calculated values of k_{31}, k_{32},k_{34}, k_{35} and k_{45} as functions of $\Delta\epsilon$, where k_{45} may be taken as a reference. It shows that the values of k_{3j} are zero at small $\Delta\epsilon$. At $\Delta\epsilon \geq 0.3$, the values of k_{3j} increases with $\Delta\epsilon$. In particular, k_{31} and k_{32} are much larger than k_{34} and k_{35}, which indicates that the edge state is coupled strongly to the lowest two bands, in consistency with results in Fig. 3(a).

4.2. *Phenomenological model with anti-crossing*

The emergence of edge state in Fig. 3 is mainly due to left waveguide chain with a long band end as indicated by the dashed rectangle in the insert of Fig. 3(b), thus we can choose such chain with 3 waveguides to make the coupled system further simpler. In Figs. 4(a) and 4(b), we obtain the band dispersion of three waveguides with COMSOL, marked as blue circles, in which there exist three bands and the edge state is coupled with bulk state in the form of anti-crossing. Similar to Fig. 3(c), Fig. 4.1(c) sketches two kinds of mode evolution of the intersection between two modes. In Fig. 4.1(c), (1) shows that two modes cross each other without coupling, and (2) shows that they are coupled with each other yielding anti-crossing, which is the same as the edge state coupled with the bulk state of lower band in Fig. 3(a). Therefore, the coupling of the three waveguides can be separated into two different mechanisms: one is the coupling between the supermodes induced by the perturbation from the local PT-symmetric condition, the other is the coupling between the edge states with the supermodes with smaller modal index. Phenomenologically, the Hamiltonian of those three waveguides system can been written as

$$H = \begin{bmatrix} \beta_{odd} & iV_1 & 0 \\ iV_1 & \beta_{even} & iV_2 \\ 0 & iV_2 & \beta_{single} \end{bmatrix}, \tag{3}$$

where β_{odd} and β_{even} are eigenvalues of the odd and even modes of two waveguides with short bond and without gain and losses respectively, $\beta_{odd} = 1.57$, $\beta_{even} = 1.47$, while β_{single}

Optics EXPRESS

is eigenvalue of the mode in single-mode waveguide without gain and losses, $\beta_{single} = 1.51$. V_1 and V_2 are the mode coupling parameters which relate to the value of $\Delta\epsilon$. Since the edge state has no reaction with bulk state out of the region $\Delta\epsilon \in [0.29, 0.34]$, the value of V_2 is negligibly small and can be ignored, while inside of this region we can choose a reference point and linearly fit the trend of V_2 as a function of $\Delta\epsilon$. Thus by parameter fitting, we can obtain $V_1 = 0.157\Delta\epsilon$, $V_2 = \begin{cases} -0.068\Delta\epsilon + 0.023 + (-0.043\Delta\epsilon + 0.012)i & \Delta\epsilon \in [0.29, 0.34], \\ 0 & \Delta\epsilon \notin [0.29, 0.34] \end{cases}$. Plugging these parameter in Eq. (3), we obtain mode coupling of three waveguides system as sketched in the inset on the top of Fig. 4.1(b), which are plotted in Figs. 4(a) and 4(b) marked as red dots. And the results are consistent with those from COMSOL. From Eq. (3), it is shown directly that the edge state is coupled with bulk state in the lower band, but there is no direct interaction with the bulk state in the upper band.

5. Conclusion

We give a detailed examination of bulk state in a dimerized PT symmetric waveguide lattice with infinite periods, as well as the properties of the edge state in a finite dimerized PT symmetric waveguide chain in non Hermitian settings. In the Hermitian limit, we find that the bulk states have real eigenvalues, and the topological invariant associated with each band admits either 0 or π, which resembles SSH model. Consequently, the edge state can be formed at the interface, where two topologically different waveguide chains are combined. Further, we find that the edge state can exist in both global PT-symmetric and local PT-symmetric structures. The existence of edge state is ensured by the sub-lattice PT-symmetry, though the edge state in global PT-symmetric structure is more robust. As the non-Hermiticity increases, we find that the edge state can strongly couple to the bulk states from the lower band. It is due to the particular geometric configuration of waveguide lattice that shifts the band center in the band diagram upwards. Consequently, the shifts lead to inevitable crossing between the edge state and the lower bands. We further examine the strong coupling of the edge state to lower band states using non-Hermitian coupled mode theory, as well as phenomenological model. Indeed, both approaches indicate a significant interaction between the edge state and the bulk states, which leads to a strong hybridization between the edge state and the bulk states. We envisage that the strong hybridization may be useful for mode conversion between bulk and edge states in non-Hermitian settings.

Funding

National Natural Science Foundation of China (NSFC) (Grant No. 61405067, 61405066 and 61275201); Foundation for Innovative Research Groups of the Natural Science Foundation (NSF) of Hubei Province (Grant No. 2014CFA004); Research Grants Council (RGC), University Grants Committee (UGC), Hong Kong (AoE/P -02/12).